Quantitative Analysis of Tetrapentylammonium-Induced Blockade of Open N-Methyl-D-Aspartate Channels

Alexander I. Sobolevsky
Institute of General Pathology and Pathophysiology, Baltiyskaya 8, 125315, Moscow, Russia

ABSTRACT The blockade of open N-methyl-d-aspartate (NMDA) channels by tetrapentylammonium (TPentA) in acutely isolated rat hippocampal neurons was studied using whole-cell patch-clamp techniques. TPentA prevented the closure of the NMDA channel following what is known as the foot-in-the-door mechanism. Hooked tail currents appearing after termination of the agonist (aspartate) and TPentA coapplication were analyzed quantitatively according to the corresponding sequential kinetic model. Studies of the hooked tail current amplitude and the degree of the stationary current inhibition dependence on the blocker concentration led to a new method for estimation of fast foot-in-the-door blocker binding/unbinding rate constants. The application of this method to the NMDA channel blockade by TPentA allowed finding the values of its binding (1.48 $\mu M^{-1}s^{-1}$) and unbinding (14 s^{-1}) rate constants. An analysis of the dependence of the electric charge carried during the hooked tail current on the blocker concentration led to a new method for estimation of the maximum NMDA channel open probability, P_0. The value of P_0 found in experiments with TPentA was 0.04.

INTRODUCTION

Unique properties, such as high Ca^{2+} permeability (MacDermott et al., 1986), voltage-dependent Mg^{2+} block (Nowak et al., 1984), and slow activation kinetics (Johnson and Ascher, 1987; Lester et al., 1990), as well as complex regulation of NMDA channels, underlie their implication in synaptic plasticity and development, learning, and memory, as well as a variety of pathological processes occurring in the brain (McBain and Mayer, 1994; Dingledine et al., 1999). The important physiological role of NMDA channels explains the broad interest in their properties, structure, and regulation. Identification of the NMDA channel blocking mechanisms is important not only because the blockers are used in the clinical practice for treatment of a variety of neurological disorders (Danysz and Parsons, 1998; Parsons et al., 1998, 1999), but also because they proved to be one of the most effective tools in the study of the gross architecture of NMDA channels (Koshelev and Khodorov, 1992, 1995; Subramaniam et al., 1994; Benveniste and Mayer, 1995; Zarei and Dani, 1995; Antonov et al., 1998; Sobolevsky and Koshelev, 1998; Sobolevsky et al., 1998, 1999a,b; Antonov and Johnson, 1999; Sobolevsky, 1999).

According to their action on NMDA channel gating, all blockers can be subdivided into two main groups: those that prevent the channel closure and those that do not prevent it. The latter group, or the group of trapping blockers, includes MK-801, phencyclidine, NEFA, ketamine, aminoadamantanes, *N*-2-(adamantyl)-hexamethylenimine (A-7), tetramethylammonium, tetrapropylammonium and Mg^{2+} (MacDonald et al., 1987, 1991; Huetter and Bean, 1988; Johnson et al., 1995; Blanpied et al., 1997; Chen and Lipton, 1997; Dilmore and Johnson, 1998; Sobolevsky et al., 1998, 1999b; Sobolevsky and Yelshansky, 2000). In contrast, the blockers such as 9-aminoacridine, tacrine, long-chain adamantane derivatives, and tetrapentylammonium (Koshelev and Khodorov, 1992, 1995; Costa and Albuquerque, 1994; Vorobjev and Sharonova, 1994; Antonov et al., 1995, 1998; Benveniste and Mayer, 1995; Johnson et al., 1995; Antonov and Johnson, 1996; Sobolevsky, 1999; Sobolevsky et al., 1999b) are thought to prevent the closure of the channel activation gate according to the "foot-in-the-door" mechanism. All currently known foot-in-the-door blockers show relatively fast binding/unbinding kinetics. To describe this kinetics, single-channel rather than whole-cell recordings were extensively used (Costa and Albuquerque, 1994; Nelson and Albuquerque, 1994; Antonov et al., 1995, 1998; Johnson et al., 1995; Antonov and Johnson, 1996). Using TPentA as an example, this study provides a quantitative description of fast foot-in-the-door blocker binding/unbinding kinetics based solely upon whole-cell recordings.

Another important question considered in the present study is the estimation of the maximum NMDA channel open probability, P_0. Both trapping (MK-801: Huetter and Bean, 1988; Jahr, 1992; Hessler et al., 1993; Rosenmund et al., 1995; Dzubay and Jahr, 1996; Chen et al., 1999) and foot-in-the-door blockers (9-aminoacridine: Benveniste and Mayer, 1995; Chen et al., 1999) were used to determine the value of P_0. However, both MK-801 and 9-aminoacridine methods have a number of disadvantages (Benveniste and Mayer, 1995; Dilmore and Johnson, 1998). This study presents an alternative method for P_0 estimation. The application of this method to the TPentA-induced blockade revealed rather a low value of the maximum NMDA channel open probability, $P_0 \sim 0.04$.

MATERIALS AND METHODS

Pyramidal neurons were acutely isolated from the CA-1 region of rat hippocampus using vibrodissociation techniques (Vorobjev, 1991). The

Received for publication 17 November 1999 and in final form 16 May 2000.

Address reprint requests to Alexander I. Sobolevsky, Department of Neurobiology and Behavior, State University of New York at Stony Brook, Stony Brook, NY 11794-5230. Tel.: 631-632-4406; Fax: 631-632-6661; E-mail: asobolevsky@notes2.cc.sunysb.edu.

0006-3495/00/09/1324/12 $2.00

experiments were begun after 3-hour incubation of hippocampal slices in a solution containing NaCl, 124 mM; KCl, 3 mM; $CaCl_2$, 1.4 mM; $MgCl_2$, 2 mM; glucose, 10 mM; $NaHCO_3$, 26 mM. The solution was bubbled with carbogen at 32°C. During the whole period of isolation and current recording, nerve cells were washed with a Mg^{2+}-free 3 μM glycine-containing solution of NaCl, 140 mM; KCl, 5 mM; $CaCl_2$, 2 mM; glucose, 15 mM; HEPES, 10 mM; pH 7.3. Fast replacement of superfusion solutions was achieved by using the concentration-jump technique (Benveniste et al., 1990a; Vorobjev, 1991) with one application tube. This technique allows substitution of the tubular for the flowing solution with a time constant smaller than 30 ms but backward with the time constant of 30 to 100 ms (Sobolevsky, 1999). Therefore, except where noted (Fig. 8 *A*), the rate of the solution exchange was fast at the beginning of any application and slightly slower at its termination. The currents were recorded at 18°C in the whole-cell configuration using micropipettes made from pyrex tubes and filled with an intracellular' solution of CsF, 140 mM; NaCl, 4 mM; HEPES, 10 mM; pH 7.2. The electric resistance of the filled micropipettes was 3 to 7 MΩ. Analogue current signals were digitized at 2 kHz and filtered at 1 kHz frequency. The magnitude of the junction potential was about 4 mV irrespective of the presence of TPentA in the external solution. No correction for the junction potential was made because of its negligibility in comparison with the value of the holding membrane potential (−100 mV) at which all experiments were carried out.

Statistical analysis was performed using the scientific and technical graphics computer program Microcal Origin (version 4.1 for Windows). The data presented are means ± SE; a comparison of the means was done byanalysis of variance, with $p < 0.05$ taken as significant.

The dependencies of the degree of the stationary current inhibition, $1 - I_B/I_C$ (where I_C and I_B are the stationary control and blocked currents, respectively; see Fig. 1 *A*), the normalized charge carried during the tail current, Q, and the amplitude of the hooked tail current, $(I_P - I_B)/I_C$ (where I_P is the maximum value of the hooked tail current; see Fig. 1 *A*), on the blocker concentration were fitted by the following logistic equation:

$$F([B]) = \frac{A_1 - A_2}{1 + ([B]/[B]_0)\hat{}p} + A_2 \qquad (1)$$

where $F([B])$ is $1 - I_B/I_C$, Q, or $(I_P - I_B)/I_C$; A_1 and A_2 are the minimum and maximum values of $F([B])$, respectively; [B] is the blocker concentration; $[B]_0$ is the blocker concentration resulting in 50% effect, and p is the Hill coefficient describing the steepness of the fit.

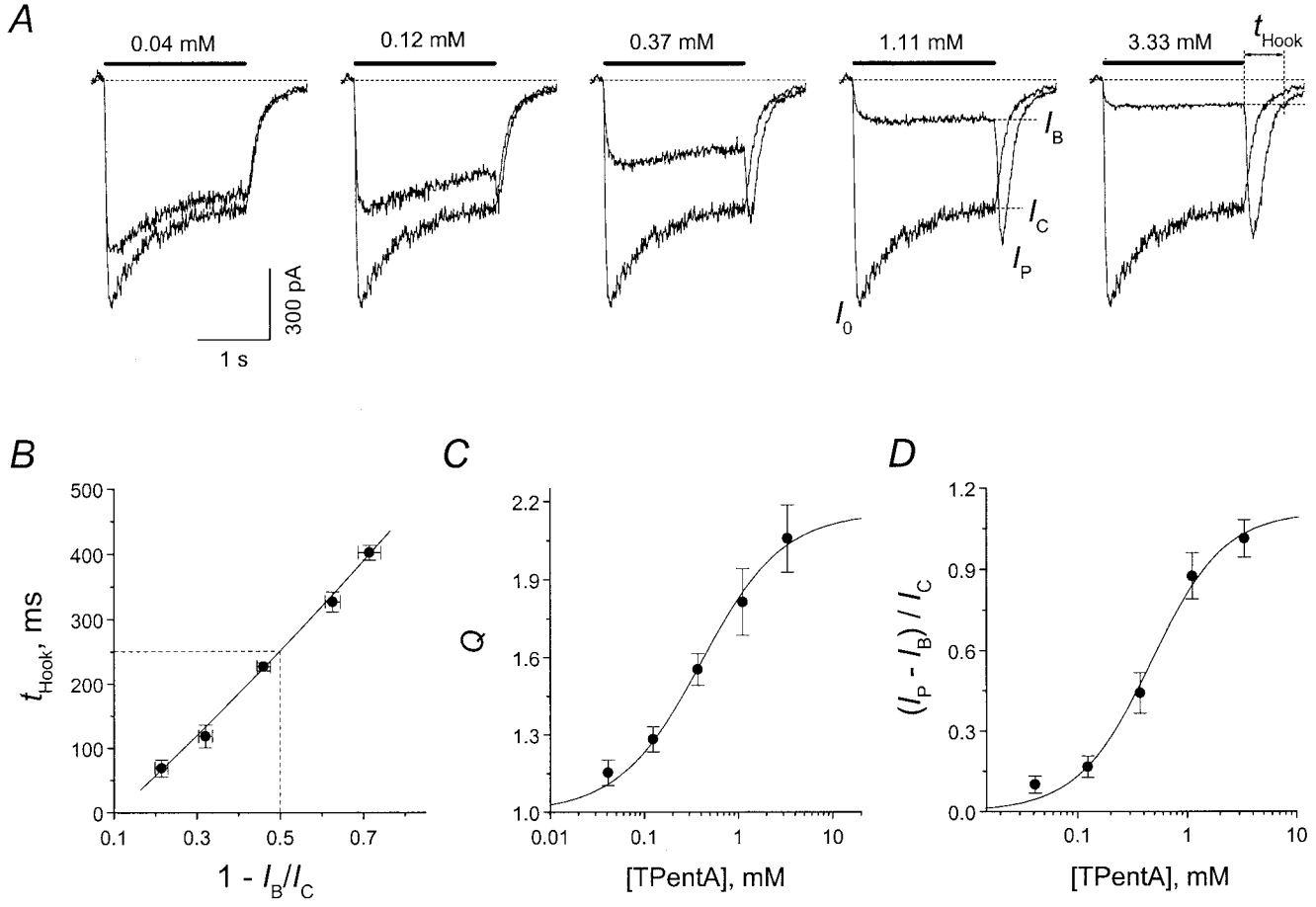

FIGURE 1 The dependencies of the hooked tail current parameters on TPentA concentration. (*A*) Superposition of control and blocked currents at different concentrations of TPentA. ASP (100 μM) was applied for 2 s alone or with TPentA (0.04, 0.12, 0.37, 1.11, or 3.33 mM). (*B*) The dependence of duration of the hooked tail current, t_{Hook}, measured at the level of the stationary blocked current, I_B, on the degree of the stationary current inhibition, $1 - I_B/I_C$. The *solid line* shows the parabolic fit. The *vertical dashed line* corresponds to $1 - I_B/I_C = 0.5$. The *horizontal dashed line* corresponds to $t_{Hook} =$ 254 ms. (*C*) The dependence of the normalized charge carried during the hooked tail current, Q, on TPentA concentration. The *solid line* is the fit of the Q dependence by Eq. 1 with $A_1 = 1$, $A_2 = 2.16 \pm 0.08$, $p = 1.01 \pm 0.23$, and $[B]_0 = 0.40 \pm 0.12$ mM ($n = 7$). (*D*) The dependence of the amplitude of the hooked tail current, $(I_P - I_B)/I_C$, on TPentA concentration. The *solid line* is the fit of the $(I_P - I_B)/I_C$ dependence by Eq. 1 with $A_1 = 0$, $A_2 = 1.11 \pm 0.10$, $p = 1.30 \pm 0.26$, and $[B]_0 = 0.47 \pm 0.10$ mM ($n = 7$).

The kinetic model used to simulate the blocking action of TPentA was based on the conventional rate theory and used independent forward and reverse rate constants to simultaneously solve first-order differential equations representing the transitions between all possible states of the channel. The processes of NMDA channels activation, opening, and desensitization were described in accordance with a kinetic model proposed by Lester and Jahr (1992). The kinetic constants for the agonist binding, $l_1 = 2\ \mu M^{-1}s^{-1}$, and unbinding, $l_2 = 25\ s^{-1}$, were taken to be approximately the same as those determined for NMDA (Benveniste and Mayer, 1991). The choice of the value of the NMDA unbinding rate constant for aspartate can be justified by the striking similarity in the kinetics of the current decay after short-term NMDA and aspartate applications (Lester and Jahr, 1992). The applicability of the NMDA binding rate constant to aspartate follows from the fact that EC_{50} measured in our experiments with aspartate (15.5 ± 1.1 μM, $n = 6$) is practically the same as EC_{50} predicted by Model 1 at the values of l_1 and l_2 listed above (16.1 ± 0.4 μM). The kinetic constants for the entrance into (γ) and recovery from (ϵ) desensitization, determined by the previously described method (Sobolevsky and Koshelev, 1998), were 0.93 s^{-1} and 0.82 s^{-1}, respectively. The choice of the value of the kinetic constant for the channel closure, α, was based on the studies of single NMDA channels (Ascher et al., 1988; Cull-Candy and Usowich, 1989; Jahr and Stevens, 1990). As the mean open time in these studies varied from 2.5 to 7 ms, the value of 200 s^{-1} was taken for α. Therefore, with the exception of the rate constant of the channel opening, β, each rate constant for the NMDA channel activation scheme (Lester and Jahr, 1992) can be estimated within a short range of magnitude. In contrast, indirect methods of estimation of β, which cannot be measured directly, gave extremely scattered values. Thus, the value of the maximum NMDA channel open probability, $P_0 = \beta/(\alpha + \beta)$, which at a given α is mutually dependent on β, was estimated in different studies in a wide range of 0.025 to 0.520 (Jahr, 1992; Hessler et al., 1993; Benveniste and Mayer, 1995; Rosenmund et al., 1995; Dzubay and Jahr, 1996; Chen et al., 1999). Due to this large scatter in values, the initially unknown value of β was estimated in the present study.

The solution exchange was assumed to be a single-exponential process (Benveniste et al., 1990b). The time constant of the solution exchange at the beginning of the agonist and the blocker coapplication measured by the method of sodium concentration jumps (Vyklicky et al., 1990; Chen and Lipton, 1997) varied in a wide range of 5 to 25 ms and in the modeling experiments was accepted as 10 ms. The initially unknown values of the time constant of the solution exchange at termination of the agonist and the blocker coapplication, τ_{wash}, as well as the rate constants of the blocker binding and unbinding, k_{on} and k_{off}, respectively, were estimated. Up to the moment of estimation, the value of k_{on} was taken arbitrarily (3.5 $\mu M^{-1}s^{-1}$ as for tetrabutylammonium in the previous study by Sobolevsky, 1999) but the blocker concentration was measured in the values of the microscopic $K_d = k_{off}/k_{on}$.

Differential equations were solved numerically using the algorithm analogous to that described previously (Benveniste et al., 1990b).

Tetrapentylammonium was purchased from Aldrich (Milwaukee, WI).

RESULTS

Ionic currents through NMDA channels were elicited by fast application of 100 μM aspartate (ASP) in a Mg^{2+}-free, 3 μM glycine-containing solution. At the holding potential of −100 mV, ASP induced an inward current that, after an initial fast rise ($\tau < 30$ ms) up to the value, I_0, indicating the opening of NMDA channels, decreased gradually (τ_D = 570 ± 25 ms, $n = 7$) down to a certain plateau level, I_C (Fig. 1 *A*). Such a current decay under the continuing action of the agonist is considered to be the result of desensitization of the receptor-channel complex. The fraction of desensitized channels, $d = 1 - I_C/I_0$, was, on average, 0.44 ± 0.06 (n = 7). TPentA inhibited the ASP-induced currents in a concentration-dependent manner with both the initial and the stationary currents decreased with an increase in the TPentA concentration (Fig. 1 *A*). The dependence of the degree of the stationary current inhibition ($1 - I_B/I_C$) on the blocker concentration was well fitted by Eq. 1 (not shown). The parameter A_1 was fixed at 0 (when TPentA concentration, [B] = 0, the current inhibition was absent). The value of A_2 when this parameter was left free proved to be indistinguishable from 1 (1.00 ± 0.11, $n = 7$). As this value is predicted by kinetic modeling (see Eq. 2 below), A_2 was fixed at 1 in order to minimize the errors for the varied parameters. The values of the varied parameters were as follows: $p = 0.55 \pm 0.04$ and $IC_{50} = [B]_0 = 0.54 \pm 0.05$ mM ($n = 7$).

The termination of each agonist and blocker coapplication was followed by a transient increase in the inward current (hooked tail current) that was absent when ASP was applied alone (Fig. 1 *A*). The duration of the hooked tail current, t_{Hook}, measured starting from the beginning of the solution exchange at the level of the stationary blocked current, I_B, increased almost linearly with an increase in the degree of stationary current inhibition, $1 - I_B/I_C$, but was better fitted by a parabola (Fig. 1 *B*). The value of t_{Hook} corresponding to 50% stationary current inhibition, t_{Hook}^{50}, was 254 ± 9 ms ($n = 7$).

The electrical charge (measured by integrating the current curve starting from the beginning of the solution exchange) carried during the hooked tail current, Q_{hook}, was higher than that carried during the control tail current, $Q_{control}$. Their ratio, $Q = Q_{hook}/Q_{control}$, increased with an increase in the TPentA concentration. The dependence of Q on the TPentA concentration was well fitted by Eq. 1 at fixed A_1 = 1 (when the TPentA concentration, [B] = 0, the control and blocked currents coincide and, correspondingly, $Q = 1$). The values of the varied parameters were as follows: A_2 = 2.16 ± 0.08, $p = 1.01 \pm 0.23$, and $[B]_0 = 0.40 \pm 0.12$ mM ($n = 7$; Fig. 1 *C*).

The amplitude of the hooked tail current, $(I_P - I_B)/I_C$, also increased with TPentA concentration. The $(I_P - I_B)/I_C$ dependence on the TPentA concentration was well fitted by Eq.1 at fixed $A_1 = 0$ (when TPentA concentration, [B] = 0, the control and blocked currents coincide and, correspondingly, the hooked tail current is absent). The values of the varied parameters were as follows: $A_2 = 1.11 \pm 0.10$, p = 1.30 ± 0.26, and $[B]_0 = 0.47 \pm 0.10$ mM ($n = 7$; Fig. 1 *D*).

The following model was used to simulate the blocking effect of TPentA on NMDA channels (Sobolevsky et al., 1999b):

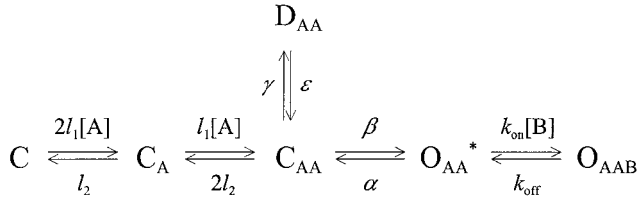

Model 1

where C, D, and O represent the channel in closed, desensitized, and open states, respectively. The subscripts A, AA, and B indicate the binding of one agonist, two agonist, and one blocker molecule to the channel, respectively, and [A] is the agonist concentration. The conducting state is marked with an asterisk.

Model 1 implies that the blocker prohibits the channel closure and, consequently, desensitization and the agonist dissociation from the blocked channel. This model predicted hooked tail currents. Their characteristics, t_{Hook}, Q and $(I_P - I_B)/I_C$, strongly depended on the unknown parameters, the time constant of the solution exchange, τ_{wash}, the rate constant of the channel opening, β, or the maximum open probability, $P_0 = \beta/(\alpha + \beta)$ (β and P_0 are mutually dependent at a given α and only P_0 will be mentioned further), and the blocker unbinding rate constant, k_{off} (Fig. 2). The hooked tail current became smaller and wider with an increase in τ_{wash} (Fig. 2 *A*). Its duration, t_{Hook}, did not change significantly with the maximum open probability, but its amplitude, $(I_P - I_B)/I_C$, decreased with P_0 (Fig. 2 *B*). $(I_P - I_B)/I_C$ increased with the blocker unbinding rate constant, whereas t_{Hook} remained approximately constant at different k_{off} (Fig. 2 *C*).

The dependencies of t_{Hook}, Q, and $(I_P - I_B)/I_C$ on τ_{wash}, P_0, and k_{off} under the conditions of Fig. 2 are shown in Fig. 3. The duration of the hooked tail current, t_{Hook}, depended strongly on τ_{wash} (Fig. 3 *A*) but did not change significantly with P_0 and k_{off} (Fig. 3, *B* and *C*). The normalized charge carried during the hooked tail current, Q, depended on both τ_{wash} and P_0 (Fig. 3, *D* and *E*) but did not change significantly with k_{off} (Fig. 3 *F*). Finally, the hooked tail current amplitude $(I_P - I_B)/I_C$, depended on all three parameters (Fig. 3, *G*–*I*).

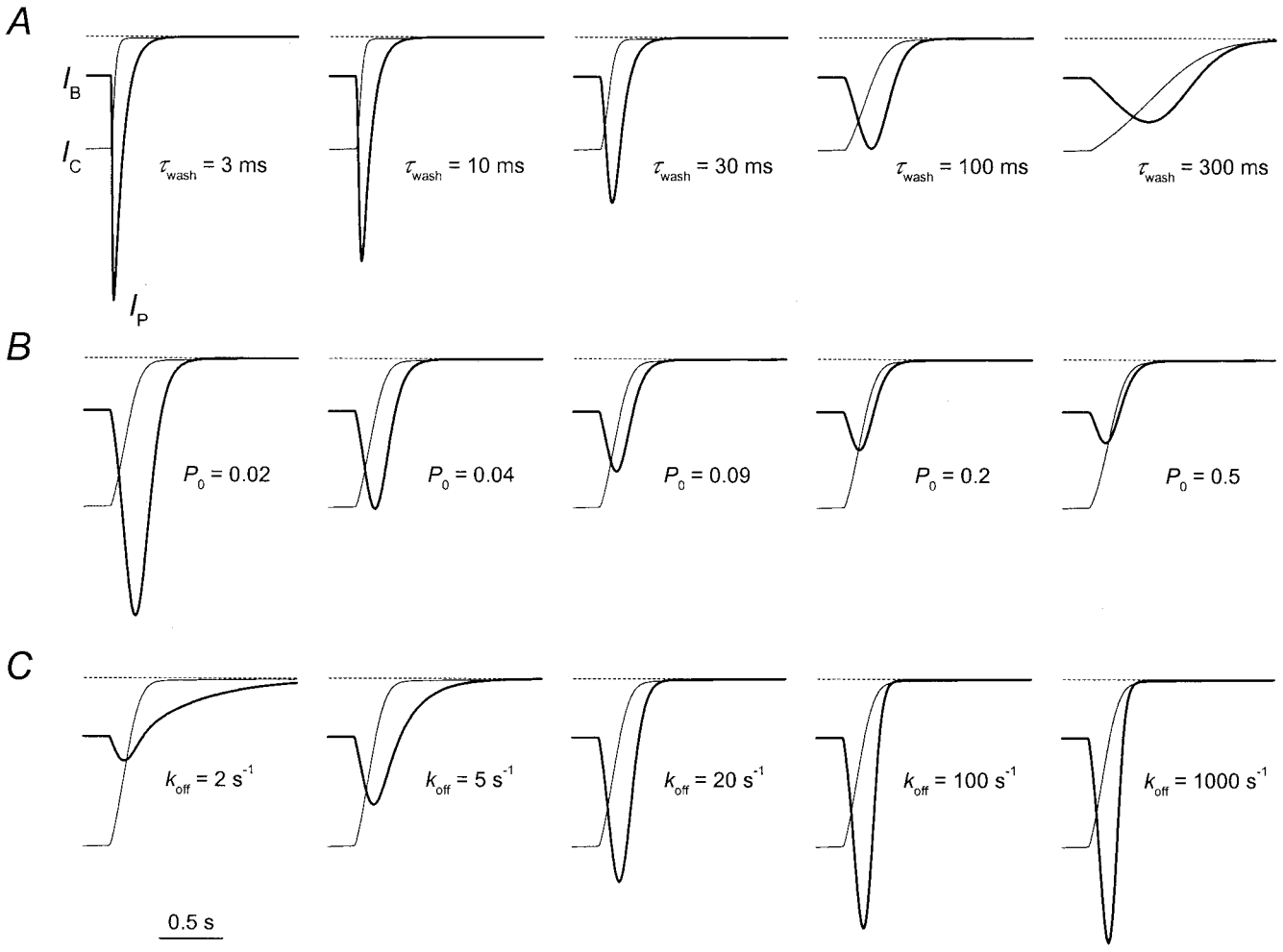

FIGURE 2 The hooked tail currents predicted by Model 1 at different values of τ_{wash}, P_0 and k_{off}. Each hooked tail current (*thick line*) is shown in a superposition with the control tail current (*thin line*). The degree of the stationary current inhibition is the same, $1 - I_B/I_C = 0.65$. The values of parameters, except where noted, were $\tau_{wash} = 70$ ms, $P_0 = 0.041$, $k_{off} = 14\ s^{-1}$, and [B] = 105 K_d. (*A*) The hooked tail currents predicted by Model 1 at different τ_{wash}. (*B*) The hooked tail currents predicted by Model 1 at different values of P_0. A smaller blocker concentration was used at higher P_0 to achieve the same degree of stationary current inhibition. Thus, at $P_0 = 0.02$, 0.04, 0.09, 0.2, and 0.5 the values of the blocker concentration, [B], were 211, 88, 45, 19, and 6 K_d, respectively. (*C*) The hooked tail currents predicted by Model 1 at different k_{off}.

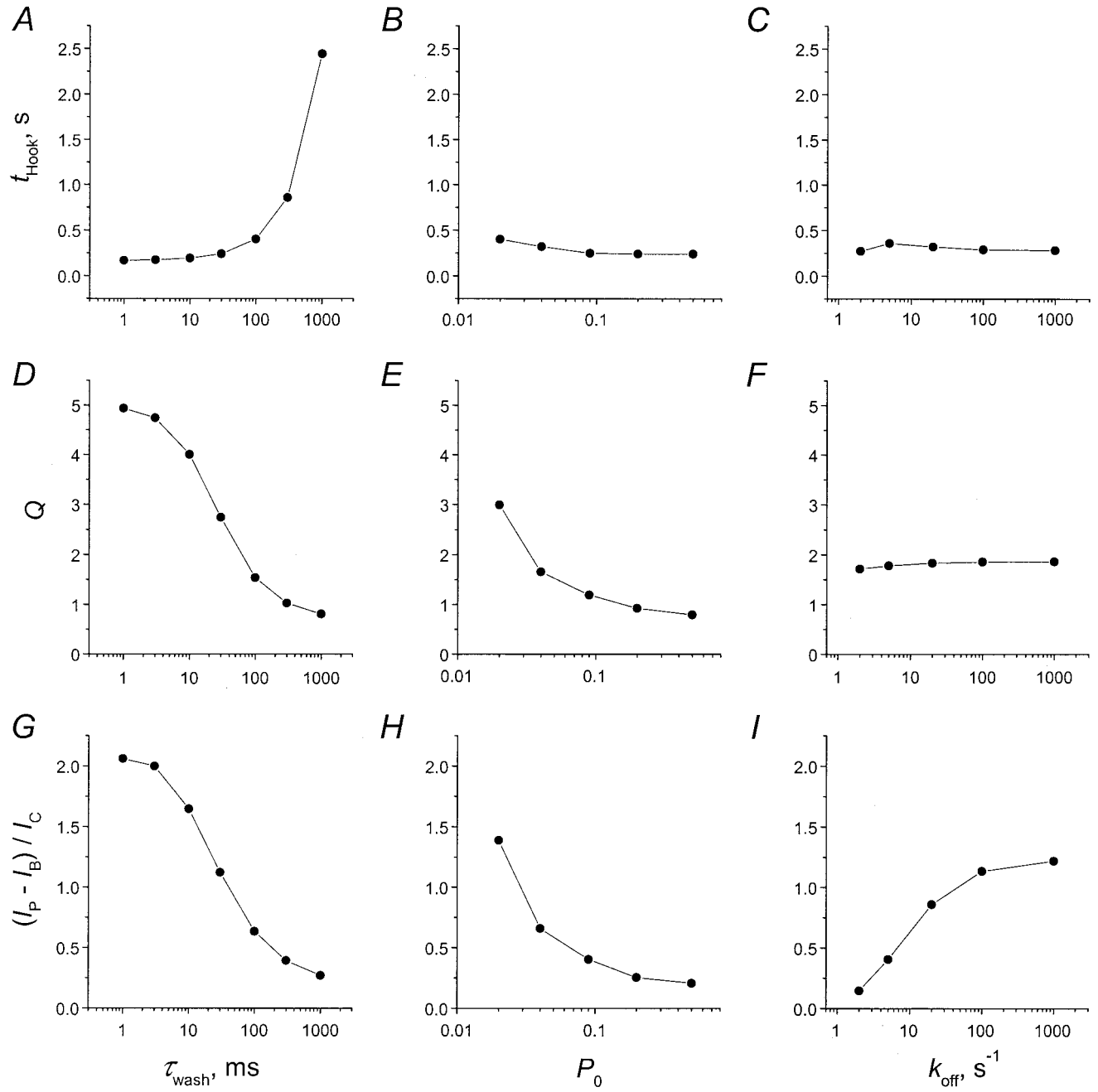

FIGURE 3 The dependencies of t_{Hook}, Q and $(I_P - I_B)/I_C$ on τ_{wash}, P_0 and k_{off} predicted by Model 1. The points connected by the lines represent the dependencies of duration of the hooked tail current, t_{Hook} (*A*, *B*, *C*), the normalized electrical charge carried during the hooked tail current, Q (*D*, *E*, *F*), and the amplitude of the hooked tail current, $(I_P - I_B)/I_C$ (*G*, *H*, *I*), on the time constant of the solution exchange, τ_{wash} (*A*, *D*, *G*), the maximum NMDA channel open probability, P_0 (*B*, *E*, *H*), and the blocker unbinding rate constant, k_{off} (*C*, *F*, *I*). The values of parameters are the same as listed in the Fig. 2 legend.

The dependencies shown in Fig. 3 permit the estimation of the unknown parameters τ_{wash}, P_0, and k_{off} by measuring t_{Hook}, Q, and $(I_P - I_B)/I_C$. Indeed, by comparing the t_{Hook} dependencies on the degree of the stationary current inhibition predicted by Model 1 at different values of τ_{wash}, one can identify the one that simulates the experimental t_{Hook} dependence (Fig. 1 *B*). The corresponding value of τ_{wash} will be an estimate of the experimental time constant of the solution exchange. At this fixed value of τ_{wash}, the Q dependencies on TPentA concentration predicted by Model 1 at different values of P_0 make it possible to establish the one that simulates the experimental Q dependence (Fig. 1 *C*). The corresponding P_0 value will be an estimate of the experimental maximum open probability. Finally, at fixed

values of τ_{wash} and P_0, the dependence of $(I_P - I_B)/I_C$ on TPentA concentration predicted by Model 1 at different values of k_{off} will permit determination of which one simulates the experimental $(I_P - I_B)/I_C$ dependence (Fig. 1 *D*). The corresponding value of k_{off} is an estimate of the experimental value of the TPentA unbinding rate constant.

The procedure described above for estimation of τ_{wash}, P_0, and k_{off} was carried out with the initial values of $P_0 = 0.09$ and $k_{off} = 1000\ s^{-1}$ used in our previous study (Sobolevsky et al., 1999b). To minimize the errors in estimation of τ_{wash}, P_0, and k_{off}, this procedure was repeated five times, each time taking the values of the parameters found in the previous iteration as initial values for the next one. The results of the second iteration did not differ significantly from those of further iterations. The results of the fifth iteration are illustrated in Figs. 4–6.

The dependence of t_{Hook} on the degree of the stationary current inhibition, $1 - I_B/I_C$, predicted by Model 1 was nearly linear at different values of τ_{wash} but was better described by a parabola (Fig. 4 *A*). The value of the duration of the hooked tail current at 50% current inhibition, t^{50}_{Hook}, increased linearly with an increase in τ_{wash} (Fig. 4 *B*). The value $\tau_{wash} = 70$ ms corresponded to the experimental value of t^{50}_{Hook} (254 ms, Fig. 1 *B*) and was within the range of τ_{wash} values (30–80 ms) estimated previously for the application system used (Sobolevsky, 1999).

The value of the normalized charge carried during the hooked tail current, *Q*, predicted by Model 1 increased with the blocker concentration and was well fitted by Eq. 1 (Fig. 5 *A*). The value of the parameter *p* changed slightly when the value of P_0 was varied. Thus, *p* increased from 1.03 at $P_0 = 0.020$ to 1.18 at $P_0 = 0.074$. In contrast, the value of the parameter A_2 strongly depended on P_0. Thus, the value of A_2 decreased from 4.01 at $P_0 = 0.020$ to 1.37 at $P_0 = 0.074$. The dependence of A_2 on P_0 was decreasing and in the range of P_0 tested was well fitted by a parabola (Fig. 5 *B*). The value $P_0 = 0.041$ corresponded to the experimental value of A_2 (2.16, Fig. 1 *C*).

The value of the amplitude of the hooked tail current, $(I_P - I_B)/I_C$, predicted by Model 1 increased with the blocker concentration and was well fitted by Eq. 1 (Fig. 6 *A*). The value of the parameter *p* was slightly different at different k_{off}: it decreased from 1.64 at $k_{off} = 2\ s^{-1}$ to 1.05 at $k_{off} = 1000\ s^{-1}$. The value of A_2 depended more strongly on k_{off}. Thus, A_2 increased from 0.38 at $k_{off} = 2\ s^{-1}$ to 1.65 at $k_{off} = 1000\ s^{-1}$. The dependence of A_2 on k_{off} was well fitted by Eq. 1 (Fig. 6 *B*). The value of $k_{off} = 14.0\ s^{-1}$ corresponded to the experimental value of A_2 (1.11, Fig. 1 *D*).

The mean outcome of the last four iterations allowed to estimate the values of the time constant of the solution exchange, $\tau_{wash} = 67 \pm 3$ ms, the maximum NMDA channel open probability, $P_0 = 0.042 \pm 0.002$, and the TPentA unbinding rate constant, $k_{off} = 14.1 \pm 0.2\ s^{-1}$. The only remaining parameter was the TPentA binding rate constant, k_{on}. It was easy to find the value of k_{on} at given k_{off} taking into account that Model 1 should simulate the effectiveness of blocking action of TPentA measured in the experiment as $IC_{50} = 0.54 \pm 0.05$ mM.

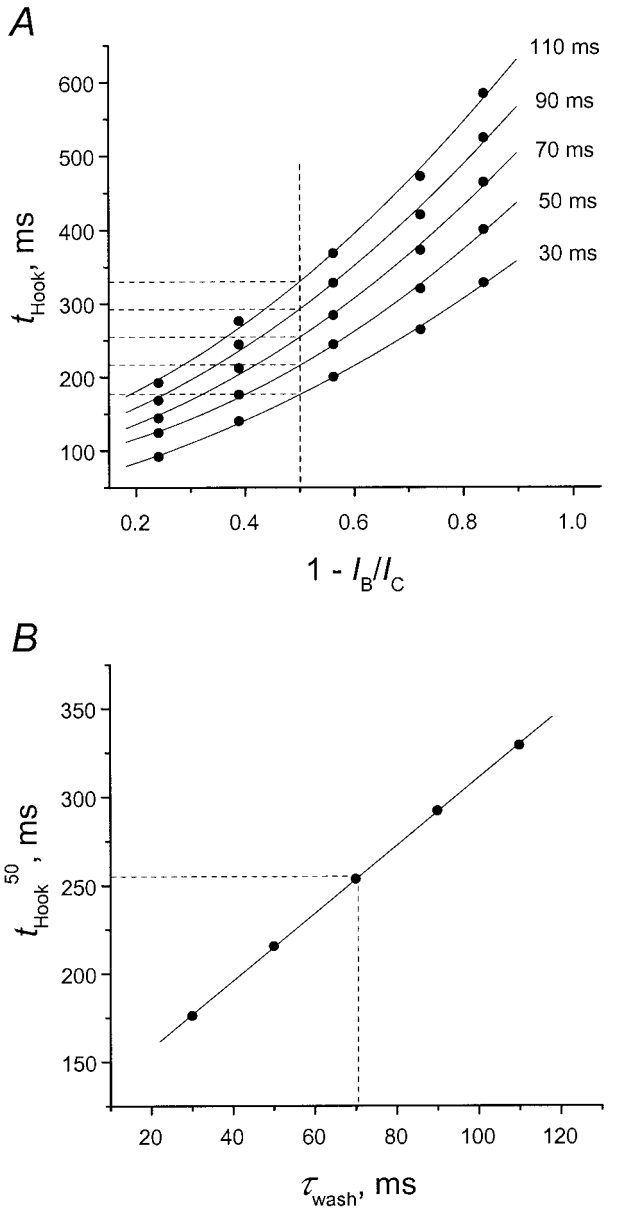

FIGURE 4 Estimation of the time constant of the solution exchange, τ_{wash}. The values of parameters $P_0 = 0.043$ and $k_{off} = 14.2\ s^{-1}$. (*A*) Dependencies of t_{Hook} predicted by Model 1 on the degree of the stationary current inhibition, $1 - I_B/I_C$, at different values of τ_{wash} (30, 50, 70, 90, and 110 ms). Each dependence was fitted by a parabola (*solid lines*). The value on a parabola at $1 - I_B/I_C = 0.5$ (*vertical dashed line*) corresponded to t^{50}_{Hook} at each τ_{wash} given (*horizontal dashed lines*). (*B*) The dependence of t^{50}_{Hook} predicted by Model 1 on τ_{wash}. The solid line shows the linear fit. The value $\tau_{wash} = 70$ ms corresponds to the experimental value of $t^{50}_{Hook} = 254$ ms (*dashed lines*).

At the values of parameters τ_{wash}, P_0, and k_{off} determined, the dependence of the stationary current inhibition, $1 - I_B/I_C$, on the blocker concentration, [B], predicted by Model

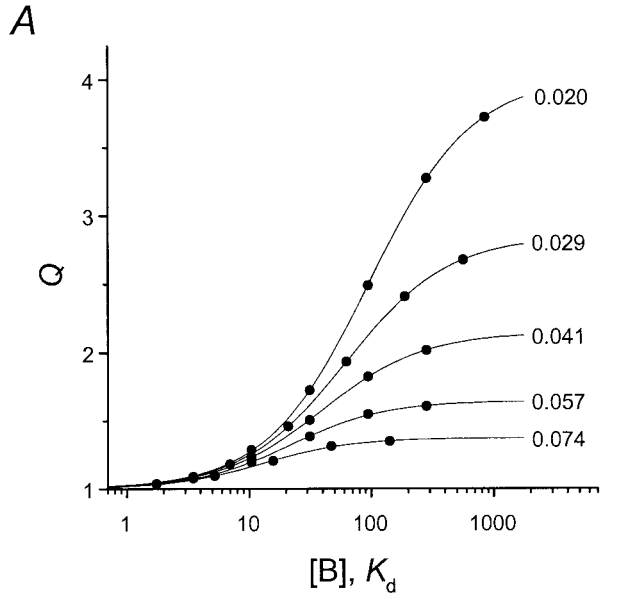

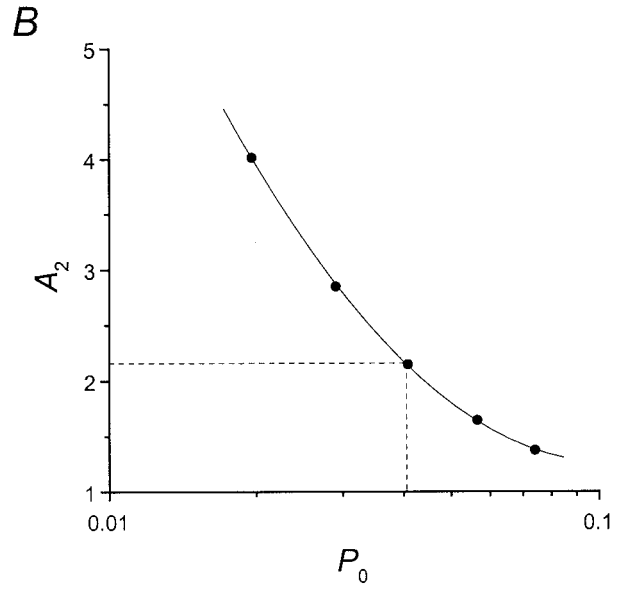

FIGURE 5 Estimation of the value of the maximum NMDA channel open probability, P_0. The values of parameters τ_{wash} = 70 ms and k_{off} = 14.2 s^{-1}. (*A*) The dependencies of the normalized charge carried during the hooked tail current, *Q*, predicted by Model 1 on the blocker concentration, [B], at different values of P_0 (0.020, 0.029, 0.041, 0.057, and 0.074). Each dependence was fitted by Eq. 1 (*solid lines*). (*B*) The dependence of the parameter A_2 value obtained from each fitting in *A* on P_0. The solid line shows the fitting of the A_2 dependence by a parabola. The value P_0 = 0.041 corresponds to the experimental value of A_2 = 2.16 (*dashed lines*).

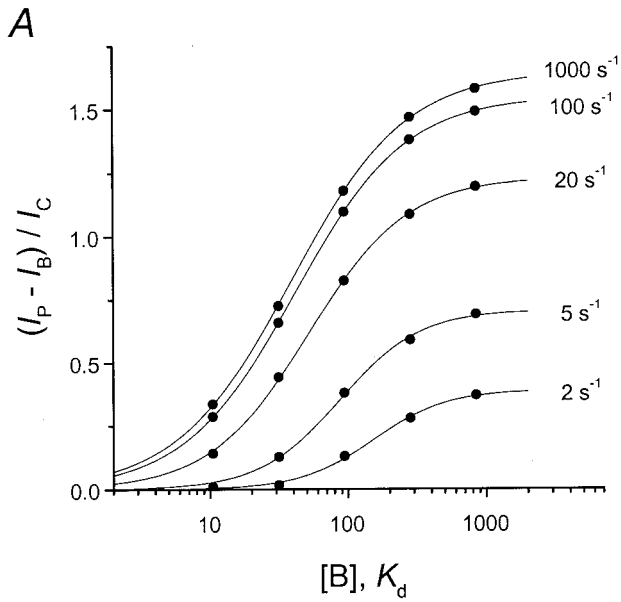

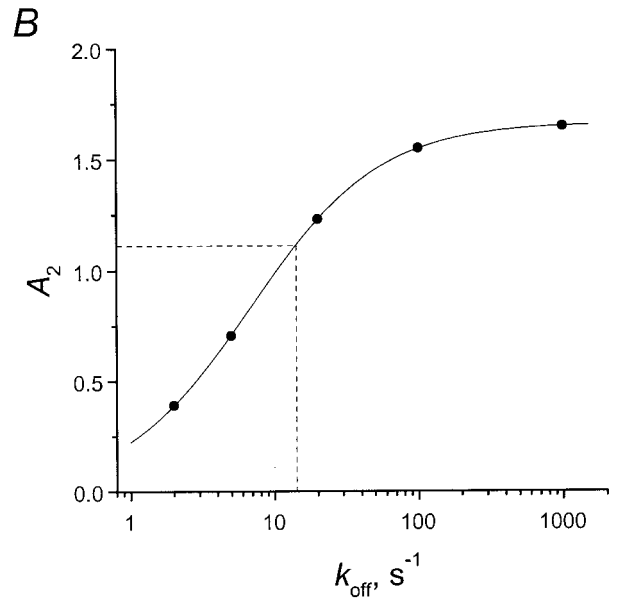

FIGURE 6 Estimation of the value of the TPentA unbinding rate constant, k_{off}. The values of parameters τ_{wash} = 70 ms and P_0 = 0.041. (*A*) The dependencies of the hooked tail current amplitude, $(I_P - I_B)/I_C$, predicted by Model 1 on the blocker concentration, [B], at different values of k_{off} (2, 5, 20, 100, and 1000 s^{-1}). Each dependence was fitted by Eq. 1 (*solid lines*). (*B*) The dependence of the value of parameter A_2 obtained from each fitting in *A* on k_{off}. The *solid line* shows the fitting of the A_2 dependence by Eq. 1. The value k_{off} = 14.0 s^{-1} corresponds to the experimental value of A_2 = 1.11 (*dashed lines*).

1 was well fitted by Eq. 1 with $A_1 = 0$, $A_2 = 1$, $p = 1.03 \pm 0.01$, and $[B]_0 = 56.7 \pm 0.1\ K_d$. To simulate the experiment, $[B]_0$ should be equal to IC_{50}, or 56.7 K_d = 56.7 k_{off}/k_{on} = IC_{50}. From the latter equality, it was easy to define the TPentA binding rate constant, k_{on} = 56.7 k_{off}/IC_{50} = 1.48 $\mu M^{-1}s^{-1}$.

At the new value of k_{on}, Model 1 predicts the concentration dependence of the stationary current inhibition with IC_{50} = 0.54 mM which is equal to the experimental one. However, the value of the Hill coefficient, $p = 1$, predicted by Model 1 (see also Eq. 2 below) is much higher than that determined experimentally, $p = 0.55 \pm 0.04$. This discrep-

ancy can be explained by the heterogeneity of the TPentA affinity due to the heterogeneity in the NMDA receptor subunit combinations expressed in the neurons under study. On the other hand, this discrepancy presumably does not reflect the heterogeneity of the mechanism of TPentA action on NMDA channels. The reason is in the striking similarity of the foot-in-the-door blockade simulated by Model 1 and that observed in the experiment. This can be clearly seen from the following tests of Model 1 at the values of parameters τ_{wash}, P_0, k_{on}, and k_{off} determined.

First, Model 1 was tested in an experiment with the agonist and the blocker coapplication (Fig. 7). The currents

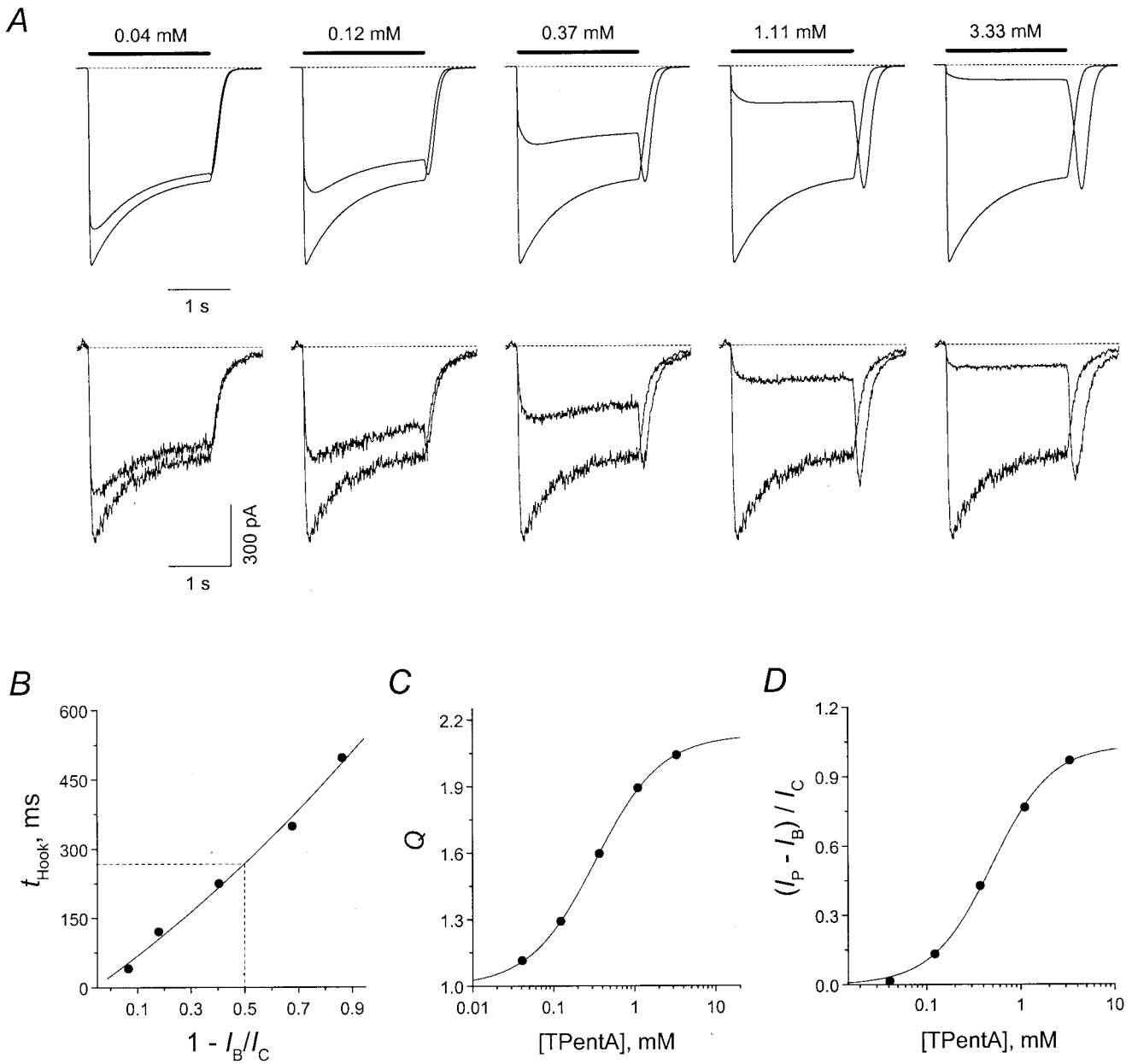

FIGURE 7 The predictions of Model 1 for the experiment with the blocker and the agonist coapplication. The values of parameters $\tau_{wash} = 70$ ms, $P_0 = 0.041$, $k_{off} = 14\ s^{-1}$, and $k_{on} = 1.48\ \mu M^{-1}s^{-1}$. (*A*) *First line*: Simulated currents at different blocker concentrations (0.04, 0.12, 0.37, 1.11, or 3.33 mM) in superposition with the simulated control current. *Second line*: Experimental currents from Fig. 1 *A*. (*B*) The dependence of t_{Hook} on the degree of stationary current inhibition, $1 - I_B/I_C$. The *solid line* shows the parabolic fit. The value $t_{Hook} = 267$ ms corresponds to the 50% stationary current inhibition (*dashed lines*). (*C*) The dependence of the normalized charge carried during the hooked tail current, Q, on the blocker concentration. The *solid line* is the fit of the Q dependence by Eq. 1 with $A_1 = 1$, $A_2 = 2.13 \pm 0.01$, $p = 1.07 \pm 0.02$, and $[B]_0 = 0.33 \pm 0.01$ mM. (*D*) The dependence of the amplitude of the hooked tail current, $(I_P - I_B)/I_C$, on the blocker concentration. The *solid line* is the fit of the $(I_P - I_B)/I_C$ dependence by Eq. 1 with $A_1 = 0$, $A_2 = 1.03 \pm 0.03$, $p = 1.37 \pm 0.10$, and $[B]_0 = 0.49 \pm 0.04$ mM.

predicted by Model 1 at different blocker concentrations (Fig. 7 *A*, first line) were very similar to those observed in the experiment with TPentA (Fig. 7 *A*, second line). The coincidence of the experimental and modeling data differs only during the recovery of the current after termination of ASP application (the experimental recovery kinetics contains a slow component which is not practically resolved in the modeling recovery). This discrepancy is not surprising because the activation model used in the present study (Lester and Jahr, 1992) is simple and cannot reproduce many of the NMDA receptor properties described in single-channel studies (Ascher et al., 1988; Cull-Candy et al., 1988; McLarnon and Curry, 1990; Howe et al., 1991; Gibb and Colquhoun, 1992). Thus, the existence of a slow component in control current relaxation can be explained, for example, by more complex NMDA receptor desensitization (Sather et al., 1992) or by infringement of the principle of independence of the binding of two agonist molecules to the receptor (Benveniste and Mayer, 1991).

Fig. 7, *B*−*D*, tests the ability of the fitting procedure to provide reasonable fits. The dependence of duration of the hooked tail current, t_{Hook}, on the degree of the stationary current inhibition, $1 - I_B/I_C$, was fitted by a parabola (Fig. 7 *B*) and the value of t_{Hook} corresponding the 50% stationary current inhibition, $t^{50}_{Hook} = 267 \pm 15$ ms, was close to that observed experimentally ($t^{50}_{Hook} = 254 \pm 9$ ms, Fig. 1 *B*).

The dependence of Q on the blocker concentration predicted by Model 1 was well fitted by Eq. 1 (Fig. 7 *C*) with the following values of parameters: $A_1 = 1$, $A_2 = 2.13 \pm 0.01$, $p = 1.07 \pm 0.02$, and $[B]_0 = 0.33 \pm 0.01$ mM, which were quite similar to those observed in the experiment ($A_1 = 1$, $A_2 = 2.16 \pm 0.08$, $p = 1.01 \pm 0.23$, and $[B]_0 = 0.40 \pm 0.12$ mM; Fig. 1 *C*).

The dependence of the amplitude of the hooked tail current on the blocker concentration predicted by Model 1 was well fitted by Eq. 1 (Fig. 7 *D*) with $A_1 = 0$, $A_2 = 1.03 \pm 0.03$, $p = 1.37 \pm 0.10$, and $[B]_0 = 0.49 \pm 0.04$ mM and was in reasonable agreement with the experimental $(I_P - I_B)/I_C$ dependence ($A_1 = 0$, $A_2 = 1.11 \pm 0.10$, $p = 1.30 \pm 0.26$, and $[B]_0 = 0.47 \pm 0.10$ mM; Fig. 1 *D*).

For further verification, Model 1 was tested in experiments which can be considered as qualitative criteria for distinguishing the fast blockers that prevent or do not prevent the channel closure, desensitization, and agonist dissociation (Sobolevsky et al., 1999b).

First, Model 1 was examined to simulate the recovery of the blocker-inhibited current in the continuous presence of the agonist (Fig. 8 *A*). Both the experimental (left trace) and simulated (right trace) recovery currents exceeded the stationary level, I_C, thus forming an "overshoot". In both cases, the falling phase of the overshoot contained the fast component reflected the closure of the unblocked channels (the transition from O^*_{AA} to C_{AA} in Model 1), and the slow component reflected channel desensitization (the transition from C_{AA} to D_{AA}). Such a two-component current recovery

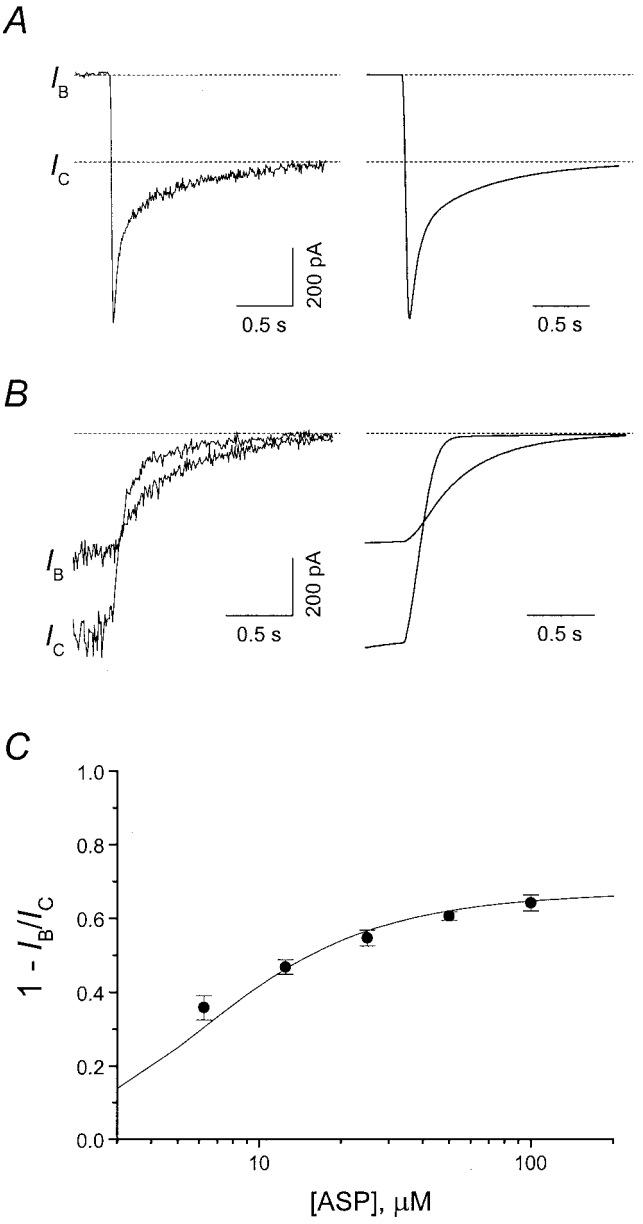

FIGURE 8 Verification of Model 1 in different experimental protocols. The values of parameters $P_0 = 0.041$, $k_{off} = 14\ s^{-1}$, and $k_{on} = 1.48\ \mu M^{-1}s^{-1}$. (*A*) Recovery of the blocker-inhibited current in the continuous presence of the agonist. *Left*: The experiment with 100 μM ASP and 3 mM TPentA. In this experiment, the faster direction of the solution exchange (see Materials and Methods) was used to remove the blocker. *Right*: Prediction of Model 1 at [B] = 3 mM and time constant of solution exchange = 10 ms. (*B*) A tail current after termination of the agonist application in the continuous presence of the blocker in superposition with the tail current after the control agonist application. *Left*: The experiment with 100 μM ASP and 0.5 mM TPentA. *Right*: Prediction of Model 1 at [B] = 0.5 mM and $\tau_{wash} = 70$ ms. (*C*) The dependence of the stationary current inhibition, $1 - I_B/I_C$, measured in the experiment with the agonist and the blocker coapplication on the agonist concentration. *Points*: Experimental data at 1 mM TPentA. *Solid line*: Prediction of Model 1 (Eq. 2) at [B] = 1 mM.

in the continuous presence of the agonist observed in the experiment with TPentA and well simulated by Model 1 is a characteristic feature of the blocker that prevents the channel closure (Sobolevsky et al., 1999b).

Model 1 was also verified in another kinetic experiment in which the tail current after the agonist application, in the continuous presence of the blocker, was compared with the control tail current (Fig. 8 *B*). In the modeling experiment (right trace) as well as in the experiment with TPentA (left trace) the control and blocked tail currents intersected. Such a delay in the current relaxation induced by the presence of the blocker in the washout solution is a characteristic feature of the blocker that prevents the agonist dissociation from the blocked channel (Sobolevsky et al., 1999b).

Finally, the ability of Model 1 to reproduce the dependence of degree of the stationary current inhibition, $1 - I_B/I_C$, on the agonist concentration was checked (Fig. 8 *C*). In the experiment with TPentA, the agonist dependence was increasing (solid circles in Fig. 8 *C*, the mean $1 - I_B/I_C$ values were significantly different, $p < 10^{-6}$, $n = 6$). Model 1 predicts the following equation for the degree of the stationary current inhibition (deduced by the previously described method; Sobolevsky, 1999):

$$1 - \frac{I_B}{I_C} = 1 - \frac{1}{1 + \dfrac{k_{on}[B]/k_{off}}{1 + (\alpha/\beta)\,[1 + (\gamma/\epsilon) + (2I_2/I_1/[A]) + (I_2/I_1/[A])^2]}} \quad (2)$$

According to Eq. 2, $1 - I_B/I_C$ increases with the agonist concentration (the solid line in Fig. 8 *C*); this prediction of Model 1 matches well the experimental points. Increasing agonist dependence, just as an intersection of tail currents in the previously described experiment, is a criterion distinguishing the blocker that prevents the agonist dissociation from the blocked channel (Sobolevsky et al., 1999b).

Thus, at the values of parameters found, all quantitative and qualitative predictions of Model 1 showed a good correspondence to the experimental data.

DISCUSSION

Model 1 proved to be a reasonable description of the TPentA-induced blockade of open NMDA channels. An analysis of characteristics of hooked tail currents generated after termination of ASP and TPentA coapplication allowed specifying all the unknown parameters of this description.

The first parameter, the time constant of the solution exchange, τ_{wash}, was found by analyzing the dependence of the hooked tail current duration, t_{Hook}, on the degree of the stationary current inhibition (Fig. 4). This method of τ_{wash} estimation is new and does not require preparation of additional experimental solutions, as is the case with sodium concentration jumps (Vyklicky et al., 1990; Chen and Lipton, 1997). The t_{Hook} method is especially convenient for application systems wherein the solution exchange varies with time (or from experiment to experiment, or from cell to cell) because it allows one to estimate τ_{wash} directly during the current recordings. Under the conditions of TPentA experiments ($P_0 = 0.04$, $k_{off} = 14\ s^{-1}$), this method is applicable if the value of τ_{wash} is higher than 10 ms (Fig. 3 *A*). The sensitivity of this method does not depend on P_0 but increases with an increase in k_{off}. Thus, at $k_{off} = 1000\ s^{-1}$, this method allows one to estimate the value of τ_{wash} if it is higher than 1 ms (not shown).

The second parameter is the maximum NMDA channel open probability, P_0, which under physiological conditions (saturating concentrations of the agonist) reflects the fraction of the total number of NMDA channels that open in response to a short pulse of the agonist. The value of P_0 was found analyzing the dependence of the normalized electric charge carried during the hooked tail current, Q, on the blocker concentration (Fig. 5) and proved to be quite low (0.04). The previous studies reported the maximum NMDA channel open probability in a wide range of 0.025 to 0.52 (Jahr, 1992; Hessler et al., 1993; Benveniste and Mayer, 1995; Rosenmund et al., 1995; Dzubay and Jahr, 1996; Chen et al., 1999). A considerable difference was observed between the values of P_0 estimated from the whole-cell current recordings (0.025–0.28) and from outside-out single-channel data (0.24–0.52; Benveniste and Mayer, 1995; Rosenmund et al., 1995). This difference can be explained by the much more rapid loss of cytoplasmic constituents that control channel gating during patch dialysis (Rosenmund et al., 1995). The P_0 value estimated in the present study (0.04) is identical to that measured by Rosenmund et al. (1995) in the whole-cell experiments.

Earlier to find P_0, in some studies the trapping blocker MK-801 was used (Huetter and Bean, 1988; Jahr, 1992; Hessler et al., 1993; Rosenmund et al., 1995; Dzubay and Jahr, 1996; Chen et al., 1999). However, the value of P_0 obtained by this method can be underestimated because of the possible overestimation of the MK-801 binding rate constant, k_{on} (Dilmore and Johnson, 1998). In other studies, 9-aminoacridine, which is believed to act as foot-in-the-door blocker, was used (Benveniste and Mayer, 1995; Chen et al., 1999). However, this method afforded only inaccurate value of P_0 for the following reasons (Benveniste and Mayer, 1995): (i) non-instantaneous recovery from block by 9-aminoacridine, (ii) space-clamp limitations, (iii) run-down for tail currents, and (iv) desensitization during the application of 9-aminoacridine. The new method for estimation of the maximum NMDA channel open probability used in the present study is applicable in the P_0 range of 0.02 to 0.5 (Fig. 3 *E*) and is devoid of the shortcomings mentioned above.

The kinetic constants of TPentA binding and unbinding, k_{on} and k_{off}, respectively, were found by analyzing the dependencies of the hooked tail current amplitude (Fig. 6) and the degree of the stationary current inhibition on the blocker concentration. The value of the unbinding rate constant, $k_{off} = 14\ s^{-1}$, attributes TPentA to rather fast blockers. The method for k_{off} estimation used in the present study is applicable for $k_{off} > 1\ s^{-1}$ (otherwise, the hook current does not appear, Fig. 2 *C*; see also Sobolevsky et al., 1999b) up to $k_{off} = 1000\ s^{-1}$ (Fig. 3 *I*).

The major limitation of the methods to estimate τ_{wash}, P_0, k_{on}, and k_{off} proposed in the present study is the so-called model dependence. Thus, these methods are applicable only to blockers that interact with NMDA channels according to the foot-in-the-door mechanism (Model 1). Even if the latter is true, the values of estimated parameters depend on fixed values of the rate constants in Model 1. Correspondingly, any inaccuracy in the definition of the rate constants l_1, l_2, γ, ϵ, or α will result in an inaccuracy of the τ_{wash}, P_0, k_{on}, and k_{off} values.

The ratio of unbinding and binding rate constants gives the apparent value of $K_d = k_{off}/k_{on} = 0.009$ mM, which is 60 times lower than $IC_{50} = 0.54 \pm 0.05$ mM. This difference between the microscopic dissociation constant (K_d) and the characteristics of the apparent affinity (IC_{50}) is due to the prevention of TPentA to the channel closure (for a trapping blocker, a blocker which does not affect the channel closure, desensitization, and agonist dissociation, $K_d = IC_{50}$). The value of the IC_{50}/K_d ratio predicted by Model 1 is equal to the denominator $1 + (\alpha/\beta)\ [1 + (\gamma/\epsilon) + (2l_2/l_1/[A]) + (l_2/l_1/[A])^2]$ in Eq. 2. From this mathematical expression, the IC_{50}/K_d ratio decreases with the agonist concentration and the maximum open probability (P_0), but increases with channel desensitization. Thus, for a blocker whose action interferes with that of the NMDA channel gating machinery, the apparent blocking strength (IC_{50}) differs considerably from its binding efficacy (K_d) and, correspondingly, the former cannot be used as an estimation of the latter.

According to Model 1, TPentA is a typical foot-in-the-door blocker, that is, when bound to the open NMDA channel it prohibits the closure of the activation gate. Therefore, the constriction of the NMDA channel pore formed by the activation gate in the closed state is most probably located in the region of the TPentA binding site. If so, the diameter of the extracellular vestibule of the NMDA channel pore in the region of the activation gate localization should not be smaller than the size of the TPentA molecule (~11 Å).

I thank Prof. B. I. Khodorov, Dr. L. P. Wollmuth, and Dr. S. G. Koshelev for comments on the manuscript and R. L. Birnova and M. V. Yelshansky for help in preparation of the manuscript. This work has been supported by the Russian Foundation for Basic Research (no. 99–04-48770) and the International Soros Science Education Program (no. a99–1650).

REFERENCES

Antonov, S. M., V. E. Gmiro, and J. W. Johnson. 1998. Binding sites for permeant ions in the channel of NMDA receptors and their effects on channel block. *Nat. Neurosci.* 1:451–456.

Antonov, S. M., and J. W. Johnson. 1996. Voltage-dependent interaction of open-channel blocking molecules with gating of NMDA receptors in rat cortical neurons. *J. Physiol.* 493:425–445.

Antonov, S. M., and J. W. Johnson. 1999. Permeant ion regulation of N-methyl-d-aspartate receptor channel block by Mg^{2+}. *Proc. Nat. Acad. Sci. USA.* 96:14571–14576.

Antonov, S. M., J. W. Johnson, N. Y. Lukomskaya, N. N. Potapyeva, V. E. Gmiro, and L. G. Magazanik. 1995. Novel adamantane derivatives act as blockers of open ligand-gated channels and as anticonvulsants. *Mol. Pharmacol.* 47:558–567.

Ascher, P., Bregestovski, P., and L. Nowak. 1988. N-methyl-d-aspartate-activated channels of mouse central neurones in magnesium-free solutions. *J. Physiol.* 399:207–226.

Benveniste, M., J. Clements, L. Vyklicky, Jr., and M. L. Mayer. 1990b. A kinetic analysis of the modulation of N-methyl-d-aspartic acid receptors by glycine in mouse cultured hippocampal neurones. *J. Physiol.* 428: 333–357.

Benveniste, M., and M. L. Mayer. 1991. Kinetic analysis of antagonist action at N-methyl-d-aspartic acid receptors: two binding sites each for glutamate and glycine. *Biophys. J.* 59:560–573.

Benveniste, M., and M. L. Mayer. 1995. Trapping of glutamate and glycine during open channel block of rat hippocampal neuron NMDA receptors by 9-aminoacridine. *J. Physiol.* 483:367–384.

Benveniste, M., J.-M. Mienville, E. Sernagor, and M. L. Mayer. 1990a. Concentration-jump experiments with NMDA antagonists in mouse cultured hippocampal neurons. *J. Neurophysiol.* 63:1373–1384.

Blanpied, T. A., F. Boeckman, E. Aizenman, and J. W. Johnson. 1997. Trapping channel block of NMDA-activated responses by amantadine and memantine. *J. Neurophysiol.* 77:309–323.

Chen, H.-S. V., and S. A. Lipton. 1997. Mechanism of memantine block of NMDA-activated channels in rat retinal ganglion cells: uncompetitive antagonism. *J. Physiol.* 499:27–46.

Chen, N., T. Luo, and L. A. Raymond. 1999. Subtype-dependence of NMDA receptor channel open probability. *J. Neurosci.* 19:6844–6854.

Costa, A. C. S., and E. X. Albuquerque. 1994. Dynamics of the actions of tetrahydro-9-aminoacridine and 9-aminoacridine on glutamatergic currents: concentration-jump studies in cultured rat hippocampal neurons. *J. Pharmacol. Exp. Ther.* 268:503–514.

Cull-Candy, S. G., J. R. Howe, and D. C. Ogden. 1988. Noise and single channels activated by excitatory amino acids in rat cerebellar granule neurones. *J. Physiol.* 400:189–222.

Cull-Candy, S. G., and M. M. Usowich. 1989. On the multiple-conductance single channels activated by excitatory amino acids in large cerebellar neurones of the rat. *J. Physiol.* 415:555–582.

Danysz, W., and C. G. Parsons. 1998. Glycine and N-methyl-d-aspartate receptors: physiological significance and possible therapeutic applications. *Pharmacol. Rev.* 50:597–664.

Dilmore, J. G., and J. W. Johnson. 1998. Open channel block and alteration of N-methyl-d-aspartic acid receptor gating by an analog of phencyclidine. *Biophys. J.* 75:1801–1816.

Dingledine, R., K. Borges, D. Bowie, and S. F. Traynelis. 1999. The glutamate receptor ion channels. *Pharmacol. Rev.* 51:7–61.

Dzubay, J. A., and C. E. Jahr. 1996. Kinetics of NMDA channel opening. *J. Neurosci.* 16:4129–4134.

Gibb, A. J., and D. Colquhoun. 1992. Activation of NMDA receptors by glutamate in cells dissociated from adult rat hippocampus. *J. Physiol.* 456:143–179.

Hessler, N. A., A. M. Shirke, and R. Malinow. 1993. The probability of transmitter release at a mammalian central synapse. *Nature.* 366: 569–572.

Howe, J. R., S. G. Cull-Candy, and D. Colquhoun. 1991. Currents through single glutamate receptor channels in outside-out patches from rat cerebellar granule cells. *J. Physiol.* 432:143–202.

Huetter, J. E., and B. P. Bean. 1988. Block of NMDA-activated current by the anticonvulsant MK-801: selective binding to open channels. *Proc. Natl. Acad. Sci. USA.* 85:1307–1311.

Jahr, C. E. 1992. High probability opening of NMDA receptor channels by l-glutamate. *Science.* 255:470–472.

Jahr, C. E., and C. F. Stevens. 1990. A quantitative description of NMDA receptor-channel kinetic behavior. *J. Neurosci.* 10:1830–1837.

Johnson, J. W., S. M. Antonov, T. S. Blanpied, and Y. Li-Smerin. 1995. Channel block of NMDA receptor. *In* Excitatory Amino Acids and Synaptic Transmission. H. V. Wheal, editor. Academic Press, Inc., London. 99–113.

Johnson, J. W., and P. Ascher. 1987. Glycine potentiates the NMDA response in cultured mouse brain neurons. *Nature.* 325:529–531.

Koshelev, S. G., and B. I. Khodorov. 1992. Tetraethylammonium and tetrabutylammonium as tools to study NMDA channels of the neuronal membrane. *Biol. Membr.* 9:1365–1369.

Koshelev, S. G., and B. I. Khodorov. 1995. Blockade of open NMDA channel by tetrabutylammonium, 9-aminoacridine and tacrine prevents channels closing and desensitization. *Membr. Cell Biol.* 9:93–109.

Lester, R., J. D. Clements, G. L. Westbrook, and C. E. Jahr. 1990. Channel kinetics determine the time course of NMDA receptor-mediated synaptic currents. *Nature.* 346:565–567.

Lester, R. A. J., and C. E. Jahr. 1992. NMDA channel behavior depends on agonist affinity. *J. Neurosci.* 12:635–643.

MacDermott, A. B., M. L. Mayer, G. L. Westbrook, S. J. Smith, and J. L. Barker. 1986. NMDA-receptor activation increases cytoplasmic calcium concentration in cultured spinal cord neurones. *Nature.* 321:519–522.

MacDonald, J. F., M. C. Bartlett, I. Mody, P. Pahapill, J. N. Reynolds, M. W. Salter, J. H. Schneiderman, and P. S. Pennefather. 1991. Actions of ketamine, phencyclidine and MK-801 on NMDA receptor currents in cultured mouse hippocampal neurons. *J. Physiol.* 432:483–508.

MacDonald, J. F., Z. Miljkovic, and P. Pennefather. 1987. Use dependent block of excitatory amino acid currents in cultured neurons by ketamine. *J. Neurophysiol.* 58:251–266.

McLarnon, J. G., and K. Curry. 1990. Single channel properties of the NMDA receptor channel using NMDA and NMDA agonists: on-cell recordings. *Exp. Brain Res.* 82:82–88.

McBain, C. J., and M. L. Mayer. 1994. N-methyl-d-aspartic acid receptor structure and function. *Physiol. Rev.* 74:723–760.

Nelson, M. E., and E. X. Albuquerque. 1994. 9-Aminoacridines act at a site different from that for Mg^{2+} in blockade of the NMDA receptor channel. *Mol. Pharmacol.* 46:151–160.

Nowak, L., P. Bregestovski, P. Ascher, A. Herbert, and A. Prochiantz. 1984. Magnesium gates glutamate-activated channels in mouse central neurones. *Nature.* 307:462–465.

Parsons, C. G., W. Danysz, and G. Quack. 1998. Glutamate in CNS disorders as a target for drug development: an update. *Drug News Perspect.* 11:523–569.

Parsons, C. G., W. Danysz, and G. Quack. 1999. Memantine is a clinically well tolerated N-methyl-d-aspartate (NMDA) receptor antagonist: a review of preclinical data. *Neuropharmacology.* 38:735–767.

Rosenmund, C., A. Feltz, and G. L. Westbrook. 1995. Synaptic NMDA receptor channels have a low open probability. *J. Neurosci.* 15: 2788–2795.

Sather, W., S. Dieudonne, J. F. MacDonald, and P. Ascher. 1992. Activation and desensitization of NMDA receptors in nucleated outside-out patches from mouse neurons. *J. Physiol.* 450:643–672.

Sobolevsky, A. I. 1999. Two-component blocking kinetics of open NMDA channels by organic cations. *Biochim. Biophys. Acta.* 1416:69–91.

Sobolevsky, A., and S. Koshelev. 1998. Two blocking sites of amino-adamantane derivatives in open N-methyl-d-aspartate channels. *Biophys. J.* 74:1305–1319.

Sobolevsky, A. I., S. G. Koshelev, and B. I. Khodorov. 1998. Interaction of memantine and amantadine with agonist-unbound NMDA-receptor channels in acutely isolated rat hippocampal neurons. *J. Physiol.* 512: 47–60.

Sobolevsky, A. I., S. G. Koshelev, and B. I. Khodorov. 1999a. Molecular size and hydrophobicity as factors which determine the efficacy of the blocking action of amino-adamantane derivatives on NMDA channels. *Membr. Cell Biol.* 13:79–93.

Sobolevsky, A. I., S. G. Koshelev, and B. I. Khodorov. 1999b. Probing of NMDA channels with fast blockers. *J. Neurosci.* 19:10611–10626.

Sobolevsky, A. I., and M. V. Yelshansky. 2000. The trapping block of NMDA receptor channels in acutely isolated rat hippocampal neurones. *J. Physiol.* 526:493–506.

Subramaniam, S., S. D. Donevan, and M. A. Rogawski. 1994. Hydrophobic interactions of n-alkyl diamines with the N-methyl-d-aspartate receptor: voltage-dependent and -independent blocking sites. *Mol. Pharmacol.* 45:117–124.

Vorobjev, V. S. 1991. Vibrodissociation of sliced mammalian nervous tissue. *J. Neurosci. Methods.* 38:145–150.

Vorobjev, V. S., and I. N. Sharonova. 1994. Tetrahydroaminoacridine blocks and prolongs NMDA receptor-mediated responses in a voltage-dependent manner. *Eur. J. Pharmacol.* 253:1–8.

Vyklicky, L., M. Benveniste, and M. Mayer. 1990. Modulation of NMDA receptor desensitization by glycine in mouse cultured hippocampal neurons. *J. Physiol.* 428:313–331.

Zarei, M. M., and J. A. Dani. 1995. Structural basis for explaining open-channel blockade of the NMDA receptor. *J. Neurosci.* 15:1446–1454.